The Prognostic Effect of Immune Cell Infiltration Depends on Molecular Subtype in Endometrioid Ovarian Carcinomas

Karolin Heinze[1,2], Evan S. Cairns[1], Shelby Thornton[2,3], Bronwyn Harris[3], Katy Milne[3], Marcel Grube[4], Charlotte Meyer[2,4], Anthony N. Karnezis[5], Sian Fereday[6,7], Dale W. Garsed[6,7], Samuel C.Y. Leung[2], Derek S. Chiu[2], Malak Moubarak[8], Philipp Harter[8], Florian Heitz[8,9], Jessica N. McAlpine[1,2], Anna DeFazio[10,11,12,13], David D.L. Bowtell[6,7], Ellen L. Goode[14], Malcolm Pike[15], Susan J. Ramus[16,17], C. Leigh Pearce[17,18], Annette Staebler[19], Martin Köbel[20], Stefan Kommoss[4], Aline Talhouk[1,2], Brad H. Nelson[2,3,17], and Michael S. Anglesio[1,2]

ABSTRACT

Purpose: Endometrioid ovarian carcinoma (ENOC) is the second most-common type of ovarian carcinoma, comprising 10%–20% of cases. Recently, the study of ENOC has benefitted from comparisons to endometrial carcinomas including defining ENOC with four prognostic molecular subtypes. Each subtype suggests differential mechanisms of progression, although tumor-initiating events remain elusive. There is evidence that the ovarian microenvironment may be critical to early lesion establishment and progression. However, while immune infiltrates have been well studied in high-grade serous ovarian carcinoma, studies in ENOC are limited.

Experimental Design: We report on 210 ENOC, with clinical follow-up and molecular subtype annotation. Using multiplex IHC and immunofluorescence, we examine the prevalence of T-cell lineage, B-cell lineage, macrophages, and populations with programmed cell death protein 1 or programmed death-ligand 1 across subtypes of ENOC.

Results: Immune cell infiltrates in tumor epithelium and stroma showed higher densities in ENOC subtypes with known high mutation burden (*POLE*mut and MMRd). While molecular subtypes were prognostically significant, immune infiltrates were not (overall survival $P > 0.2$). Analysis by molecular subtype revealed that immune cell density was prognostically significant in only the *no specific molecular profile* (NSMP) subtype, where immune infiltrates lacking B cells ($TIL_{B\ minus}$) had inferior outcome (disease-specific survival: HR, 4.0; 95% confidence interval, 1.1–14.7; $P < 0.05$). Similar to endometrial carcinomas, molecular subtype stratification was generally superior to immune response in predicting outcomes.

Conclusions: Subtype stratification is critical for better understanding of ENOC, in particular the distribution and prognostic significance of immune cell infiltrates. The role of B cells in the immune response within NSMP tumors warrants further study.

Introduction

Historically, ovarian carcinomas have been treated uniformly regardless of biological features of each histologic type, a trend that remains overwhelmingly common. In the last decade, multiple studies have shown that a standardized and molecular marker–based approach to determine the histologic subtypes of ovarian carcinoma can be helpful to correctly stratify patients and will thus result in improved reproducibility across biomarker and outcome studies of ovarian carcinoma (1–5).

Knowledge about the importance of the immune tumor microenvironment of ovarian carcinoma has been growing in the recent years; however, studies directed to ovarian carcinomas have thus

[1]Department of Obstetrics and Gynecology, University of British Columbia, Vancouver, Canada. [2]OVCARE - British Columbia's Gynecological Cancer Research Program, BC Cancer, Vancouver General Hospital, and the University of British Columbia, Vancouver, British Columbia, Canada. [3]Molecular and Cellular Immunology Core (MCIC), Deeley Research Centre, BC Cancer, Victoria, Canada. [4]Department of Women's Health, Tübingen University Hospital, Tübingen, Germany. [5]Department of Pathology and Laboratory, UC Davis Medical Center, Sacramento, California. [6]Peter MacCallum Cancer Centre, Melbourne, Victoria, Australia. [7]Sir Peter MacCallum Department of Oncology, The University of Melbourne, Parkville, Victoria, Australia. [8]Kliniken Essen Mitte, Department of Gynecology and Gynecologic Oncology, Essen, Germany. [9]Department for Gynecology with the Center for Oncologic Surgery Charité Campus Virchow-Klinikum, Charité – Universitätsmedizin Berlin, corporate member of Freie Universität Berlin, Humboldt-Universität zu Berlin, and Berlin Institute of Health, Berlin, Germany. [10]Centre for Cancer Research, The Westmead Institute for Medical Research, Sydney, New South Wales, Australia. [11]Department of Gynaecological Oncology, Westmead Hospital, Sydney, New South Wales, Australia. [12]Faculty of Medicine and Health, The University of Sydney, Sydney, New South Wales, Australia. [13]The Daffodil Centre, The University of Sydney, a joint venture with Cancer Council NSW, Sydney, New South Wales, Australia. [14]Mayo Clinic, Department of Health Science Research, Division of Epidemiology, Rochester, Minnesota. [15]Department of Epidemiology & Biostatistics, Memorial Sloan Kettering Cancer Center, New York, New York. [16]School of Clinical Medicine, UNSW Medicine and Health, University of New South Wales Sydney, Sydney, Australia. [17]Multidisciplinary Ovarian Cancer Outcomes Group (Consortium). [18]School of Public Health, University of Michigan, Ann Arbor, Michigan. [19]Institute of Pathology, University Hospital of Tübingen, Tübingen, Germany. [20]Department of Pathology, University of Calgary, Calgary, Alberta, Canada.

Corresponding Author: Michael S. Anglesio, University of British Columbia, 2660 Oak Street, OVCARE, Vancouver, British Columbia V6H 3Z6, Canada. Phone: 604-8754-111; E-mail: m.anglesio@ubc.ca

Clin Cancer Res 2023;29:3471–83

doi: 10.1158/1078-0432.CCR-22-3815

Translational Relevance

Clinical advances in practice have evolved to incorporate the molecular and mutational background of many cancers into treatment and patient management. This remains a challenge for less common cancer types that remain understudied and underrepresented in the context of utilization of molecular phenotyping data. Endometrioid ovarian carcinoma is one such entity, where combining molecular data with identification of active immune components may be useful in identifying patients that are candidates for immune checkpoint inhibitors (ICI) or other immunomodulatory therapies. Thus far, ICI strategies have been largely limited to mismatch repair–deficient tumors; however, our analysis suggests that patients in other more common subsets may benefit.

far primarily focused on high-grade serous ovarian carcinoma (HGSOC). This is justifiable given it is the most common type and responsible for the greatest mortality. Unfortunately, this has compounded poor understanding of less common histologies.

Endometrioid ovarian carcinoma (ENOC) remains one of the least understood histologic subtypes. Recently, we contributed to studies involving ENOC which showed that there is room for forecasting outcome based on the presence of immune cells. There, mild but significant overall survival benefits were observed in ENOC with higher levels of intraepithelial $CD8^+$ tumor-infiltrating lymphocytes (TIL) that also correlated with ARID1A loss (6, 7). Our group and others have taken strides in understanding the biology of ENOC, leveraging knowledge of endometrial carcinoma (8–11). ENOC accounts for approximately 10%–20% of all ovarian carcinoma cases (12–14) and are one of two endometriosis-associated ovarian carcinomas, the other being clear cell ovarian carcinoma (CCOC). ENOC arises from endometrial-type epithelium within endometriotic lesions that undergo malignant transformation (15, 16). With a shared origin of endometrial cells, ENOC tumors are histologically and molecularly similar to endometrial carcinoma, and especially endometrioid endometrial carcinomas (EEC; refs. 8–10). Both endometrial carcinoma and ENOC can be stratified into near-equivalent molecular subtypes: (i) an ultra-mutated and DNA polymerase epsilon (POLE)-mutant subgroup that has major defects in DNA proofreading repair (*POLE*mut; ref. 17); (ii) a hypermutated subgroup with DNA mismatch repair deficiencies and a microsatellite instable phenotype (MMRd); (iii) a high-copy number and p53-mutant subtype (p53abn); and (iv) a low-copy number subtype, lacking the above noted features, known as *no specific molecular profile* (NSMP)—a potentially erroneous moniker given it references only a lack of the other three profiles. Subtypes have been identified through genomics or a small number of surrogate IHC and sequencing assays (8, 18–25).

Recent successes of immunotherapy in immunologic "hot" tumor types have fueled efforts to identify ovarian carcinoma subgroups that may benefit from this new form of cancer treatment (26–28). Across many solid tumors, the density of TILs appears linked to tumor mutational burden (TMB) and the presumed accumulation of neoantigens (27). In several cancers, increasing TILs and TMB have been reported to correlate improved clinical response to immune checkpoint inhibitors (ICI; refs. 29, 30). Even in the absence of ICI-based therapy, multiple studies have shown that high rates of TILs correlate with improved outcomes in HGSOC and, to a lesser extent, ENOC (6, 7, 31, 32). Within both ovarian carcinoma and ENOC, both *POLE*mut and MMRd molecular subtypes are associated with the highest TMB (18, 25, 33, 34) and, for endometrial cancer, there is considerable evidence to support robust immune response within these (*POLE*mut and MMRd) molecular subtypes (7, 11, 35–37).

Our group recently reported the equivalency of molecular profiles present in both endometrial cancer and ENOC, wherein the genomic profile or surrogate assays can provide substantial prognostic information about four molecular subtypes (8, 18, 20, 21, 25). Similarities between ENOC and endometrial cancer suggest that pursuing medical management strategies for ENOC that are parallel to endometrial cancer/endometrioid endometrial cancer may be beneficial (38–41). Following this work, we now investigate the immune tumor microenvironment (iTME) in the context of molecular subtypes, to evaluate the potential additive prognostic value on overall survival (OS), disease-specific survival (DSS), and progression-free survival (PFS) in ENOC. This detailed understanding of immune infiltration in ENOC may highlight subsets for which ICIs are of potential benefit versus those unlikely to benefit.

We applied multiplex immunofluorescent/IHC staining to tissue microarrays representing 210 ENOC and examined the densities of different immune cell populations across tumor epithelium and associated stroma, their relationships with molecular subtype, and resulting outcome. While molecular subtypes in ENOC and endometrial cancer are near equivalent (42, 43), each disease does have unique features and we evaluated whether iTME could provide disease or subtype-specific information to ENOC that was distinct from reports in endometrial cancer (23).

Materials and Methods

Patient cohort

Our cohort consisted of a subset of previously described studies of ENOC ($n = 262$; refs. 6–8). Tissue samples from the following Canadian and German centers were used: Department of Women's Health, Tübingen University Hospital (Tübingen, Germany); Department of Gynecology and Gynecologic Oncology, Evang. Kliniken Essen-Mitte (Essen, Germany); Medizin Campus (Bodensee, Friedrichshafen, Germany); the OVCARE gynecological tissue bank (Vancouver, Canada). Research was conducted in accordance with the Canadian Tri-Council Policy Statement on Ethical Conduct for Research Involving Humans (TCPS2, 2018) which is fully compliant with the Declaration of Helsinki. In cases where patients were non-contactable, and treated more than 5 years before the start of the study, they were included under institutionally approved waiver of consent (Tübingen University Hospital Research Ethics Board). All other patients provided informed consent. Collection and use of clinical samples, and respective clinical data, was approved through local research ethics boards.

Outcome

For all Vancouver cases, the date of (debulking) surgery was set as the time of origin and the follow-up period consequentially started from this date. For the German cases, the first date of histologic proof was set as start point which mostly coincided with the debulking surgery. In rare circumstances, a diagnostic surgery preceded the main debulking surgery which were only a few days apart.

We used a "cohort wise" follow-up approach censoring observations on December 31st of each year following the year in which they had their surgery (year of diagnosis) to ensure random censoring and minimize ascertainment bias. Definitions of endpoints (OS, DSS, PFS) were as follows:

- OS: the time from surgery until the death of any cause. Patients, still alive prior to the censoring date, are censored at the time of last follow-up.
- DSS: the time from surgery until death due to ENOC. Patients, alive prior to the censoring date, or who died of an unrelated cause, are censored at the time of last follow-up. Unrelated causes of death were defined by the attending physician and/or rigorous chart review (reported cause of death) during clinical data abstraction.
- PFS: the time from surgery until there was evidence of recurrent or progressive disease (clinical evidence of recurrence, or imaging confirmation). Patients, alive and disease-free prior to the censoring date, or who died of an unrelated cause, are censored at the time of last follow-up. Unrelated causes of death were defined by the attending physician and/or rigorous chart review (reported cause of death) during clinical data abstraction.

Molecular subtyping and single-channel IHC markers

ENOC molecular subtype labels and ARID1A status were taken from previous reports on this cohort (see also **Fig. 1**; refs. 7, 8). β-Catenin, progesterone, and estrogen receptor status was assessed according to established IHC protocols wherein a portion of the Canadian cohort has been previously reported on (44–46).

Multiplex IHC panels

Multicolor IHC (mcIHC) and multispectral imaging was used to identify the iTME in epithelial and stromal compartments (23). All experiments were done on tissue microarray (TMA) platforms with samples having either 2 × 0.6 mm cores, or 3 × 0.6 mm cores. The following four costaining antibody panels were used to identify T-cell lineages (panel I) CD3/CD8/PanCK, (panel II) CD25/FoxP3/CD8/PanCK; B-cell lineages (panel III) CD20/CD79a/PanCK; and macrophages (panel IV) PD-1/PD-L1/CD68/PanCK (see below for details). PanCK staining in the above-noted panels was typically used to identify epithelial/tumor versus stromal compartments (**Fig. 2**); however, cell-specific costaining with PanCK was also used to identify populations within the panel II. For each tumor core the automated tissue segmentation and cell signal data were used to distinguish tumor and stromal compartments as well as to calculate density values for various (co-)stained cell populations. Cell phenotypes were defined by presence vs. absence of a given marker with the exception of CD25 where low and negative expression was binned (denoted as $CD25^{L-}$). For each marker panel 9%–15% of the automated data was randomly selected for validation by manual counting. To ensure representation of both epithelial and stromal cellular compartments, TMA cores were excluded when composed of < 25% (by core area) of each epithelial and stromal tissue, or when the majority of the evaluated tissue (≥95%) was recognized as stromal. When replicate cores were interpretable the mean density value was used.

Immune marker

IHC staining for the different immune marker was performed according to protocols published in Talhouk and colleagues (23).

For the B-cell lineage, IHC clone SP18 (rabbit monoclonal, Abcam) for CD79a, and clone L26 (mouse monoclonal, Biocare) for CD20 were used. For the IHC T-cell lineage, clone SP7 (rabbit monoclonal, Abcam) for CD3, clone C8/144b (mouse monoclonal, Cell Marque) for CD8, clone 4C9 (mouse monoclonal, LabVision) for CD25, and clone 236A/E7 (mouse monoclonal, Abcam) for FoxP3 were applied. For the macrophage panel, IHC was performed with clone EPR4877 (rabbit monoclonal, Abcam; ref. 2) for PD-1, clone SP142 (rabbit monoclonal, Abcam) for PD-L1, and clone SP251 (rabbit monoclonal, Abcam) for CD68. PanCK staining was generated using clone AE1/AE3+5D3 (mouse monoclonal, Biocare).

For signal detection, chromogens DAB, Warp Red, and Ferangi Blue and different fluorophores per panel (Treg:CD25–520 nm, CD8–570 nm, FoxP3–690 nm, PanCK-Coumarin; TAM: PD-1–650 nm, CD68–520, PD-L1–570 nm, PanCK-690 nm) were used.

Density of immune cell infiltrates was assessed using automated image analysis and scoring software, followed by visual confirmation. In detail, stained TMA slides were scanned with Vectra Multispectral Imaging system (PerkinElmer) and InForm 2.1 software (PerkinElmer) was utilized to quantify the immune cell populations based on a minimum of three different algorithms. InForm algorithms were initially trained on ENOC and CCOC images for spatial recognition of epithelial and stromal compartments. If neither core was assessable, data were noted as "missing" for that marker. In rare circumstances when data from only one core was assessable, those were utilized. If cases were present on multiple TMAs, average values per TMA were recorded before calculating the overall case mean.

Statistical analyses

Because average density values of several markers were zero-scored, a log (base 2) transformation was performed to received delta log

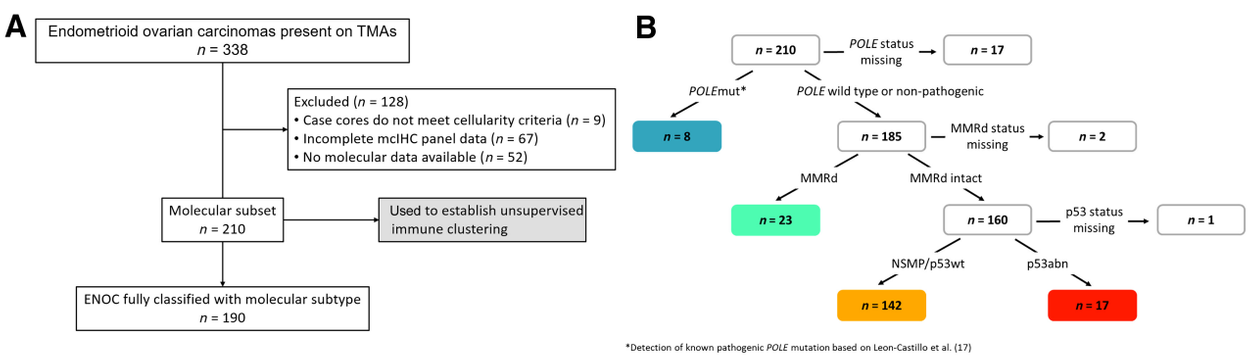

Figure 1.

Cohort classification. **A,** Schematic showing the samples included for the immune microenvironment analysis based on available data. **B,** Molecular subtype assignment of ENOC cases based on surrogate biomarkers and complete mcIHC panel data.

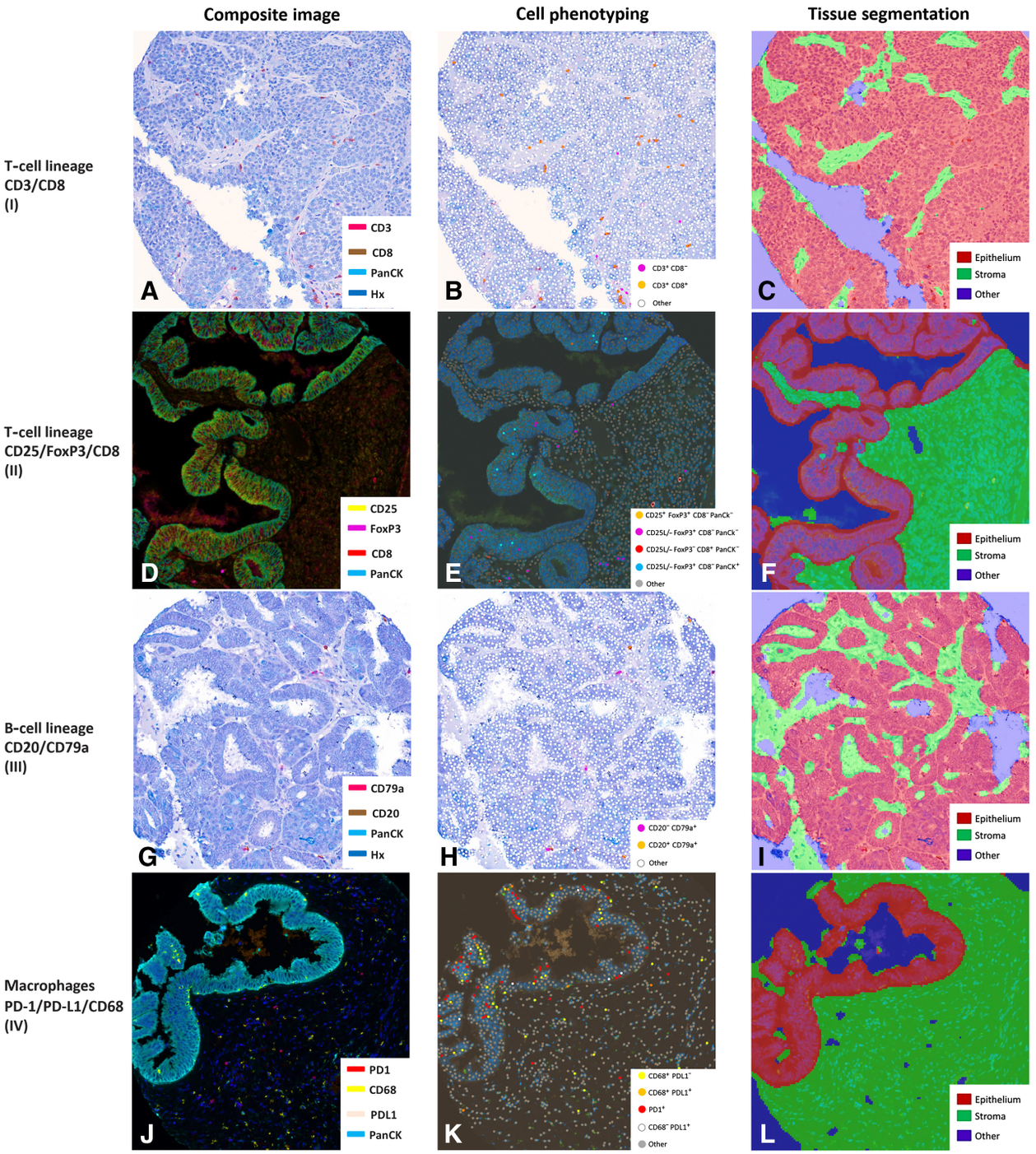

Figure 2.

Multicolor IHC. **A–L,** Representative images of multicolor IHC and multispectral imaging of TILs for each immune panel, including images of applied automated tissue segmentation into tissue compartments.

normalized data (Supplementary Fig. S1A and S1B; refs. 23, 47). Similar to published approaches (23), the immune signatures were subject to unsupervised clustering using the R package diceR (48). The final consensus clustering based on an aggregating ensemble approach was established using the k-modes method. Survival benefits in association with molecular subtypes and different immune cluster were assessed using Cox proportional hazard models and Kaplan–Meier curves with the log-rank test. R packages survival and survminer were used. Multivariable analysis was performed, correcting for the known outcome modifier: age, stage, grade, residual disease, and treatment as

well as ARID1A status and the immune clusters. Statistical significance was defined by $P < 0.05$.

Data availability

Anonymized data generated in this study are available upon request from the corresponding author. Some data may be restricted or subject to material/data transfer agreement to ensure compliance with patient consent.

Results

Cohort analysis

Of 338 ENOC cases evaluated for this study, 128 were excluded based on quality assurance or missing data. A total of 210 cases were retained with full immune profiling data and, of those, 190 had available data on molecular subtype and other biomarkers (**Fig. 1A**). Clinicopathologic cohort characteristics were consistent with our prior report (**Table 1**; ref. 8). The median age at diagnosis was 55 years. A total of 54.76% of cases were FIGO stage I, and 50.95% were grade 1. As expected, the molecular subtype distribution was 23/190 (12%) MMRd, 8/190 (4%) *POLE*mut, 17/190 (9%) p53abn, and 142/190 (75%) NSMP (**Fig. 1B**; Supplementary Table S1A). Loss of ARID1A immunoreactivity—a surrogate for loss-of-function mutations (49)—affected 52 cases (25%), including 46 with complete loss (22%) and 6 with subclonal loss (Supplementary Table S1A). As expected, ARID1A loss was most prevalent in the MMRd subtype, with 14/23 (61%), but was also observed in other subtypes with 2/8 (25%) in *POLE*mut, 29/139 (21%) in NSMP, and 1/17 (5.9%) in the p53abn subtype. Outcomes based on clinicopathologic parameters (age, stage, grade, residual disease) and the predictive value of the molecular subtypes were not different from our previous reports (Supplementary Table S1B; Supplementary Fig. S2), and similar to endometrial carcinoma (8, 20). Significant associations were seen between molecular subtype and clinicopathologic variables of grade and stage ($P = 0.018$) as well as with ARID1A status ($P < 0.001$; Supplementary Table S1C).

Table 1. Cohort characteristics.

Age	
Median	55
Mean (SD)	56.6 (13.1)
Missing	1
IQR	35.4
Stage	
I	115
II	46
III	27
IV	10
Missing	12
Grade	
1	107
2	60
3	37
Missing	6
OS follow-up	
Median	5.1
Mean (SD)	6.04 (4.32)
DSS follow-up	
Median	5.14
Mean (SD)	6.07 (4.31)
Missing	3
PFS follow-up	
Median	4.91
Mean (SD)	5.88 (4.41)
Missing	10
Residual disease	
Any	17
None	188
Missing	5
Neoadjuvant therapy	
No	72
Yes	1
Missing	137
Postsurgical chemotherapy	
No	63
Yes	132
Missing	15
Total	
n	210

Abbreviation: IQR, interquartile range.

Distribution and prognostic influence of immune cell infiltrates in epithelial and stromal compartments

By analyzing stromal and epithelial compartments of each tumor separately, it was apparent that immune populations were not evenly spread among the two compartments or across molecular subtypes (Supplementary Table S2). Overall, immune infiltrates were less abundant in the T-lineage panel II in the epithelium than in the macrophage panel III. The detection of certain populations in different compartments correlated with outcomes. Stromal $CD25^{L-}/FoxP3^{-}/CD8^{+}$ T cells mildly but significantly corresponded with the outcome of all survival parameters (OS: HR, 0.929; $P < 0.001$; DSS: 0.917; $P < 0.001$; PFS: 0.933; $P = 0.012$; Supplementary Table S3), as did stromal plasma cells ($CD20^{+}/CD79a^{+}$) for OS (HR, 0.964; $P = 0.034$) and DSS (HR, 0.952; $P = 0.028$). In the epithelial compartment, the density level of PD-1^{+} cells (HR, 0.954; $P = 0.012$) and $FoxP3^{+}$ tumor cells ($CD25^{L-}/FoxP3^{+}/CD8^{-}/PanCK^{+}$) coincided with better OS (HR, 0.929; $P = 0.017$).

Unsupervised clustering reveals TIL patterns but no prognostic significance

In our overall cohort, we applied unsupervised clustering to the IHC dataset. The optimal number of immune clusters was determined using an unsupervised approach through the R package diceR (48). To facilitate comparison to prior reports in endometrial cancer we applied a k = 2 solution, which was determined by diceR as the optimal cluster solution for our ENOC cohort (Supplementary Fig. S1C and S1D), and the next most optimal cluster solution k = 3. These divided our cohort roughly into TIL_{high} and TIL_{low} (k = 2), or TIL_{high}, TIL_{medium}, and TIL_{low} (k = 3) clusters, respectively. Underlying or driving components of each cluster are discussed below.

The compartment-independent immune signatures/phenotypes were plotted in a grouped heat map based on cluster and molecular subtype assignments (**Fig. 3A** and **B**). For most markers, the stromal and epithelial values clustered in close proximity. The TIL_{high} cluster was characterized by higher levels across most TIL subsets, in particular regulatory ($CD25^{+}/FoxP3^{+}/CD8^{-}$) and cytotoxic T cells ($CD25^{L-}/FoxP3^{-}/CD8^{+}$ and $CD3^{+}/CD8^{+}$). In contrast, the TIL_{low} cluster had lower levels of most TIL subsets and negligible B lineage (populations marked CD20 and/or CD79a) and PD-$L1^{+}$ cell populations. Nonetheless, observable differences did not translate into distinct survival outcomes with k = 2 clustering ($P > 0.1$; **Fig. 3C**).

The three-cluster solution presented more well-defined signatures and seemed to adhere to functional groupings; therefore, further

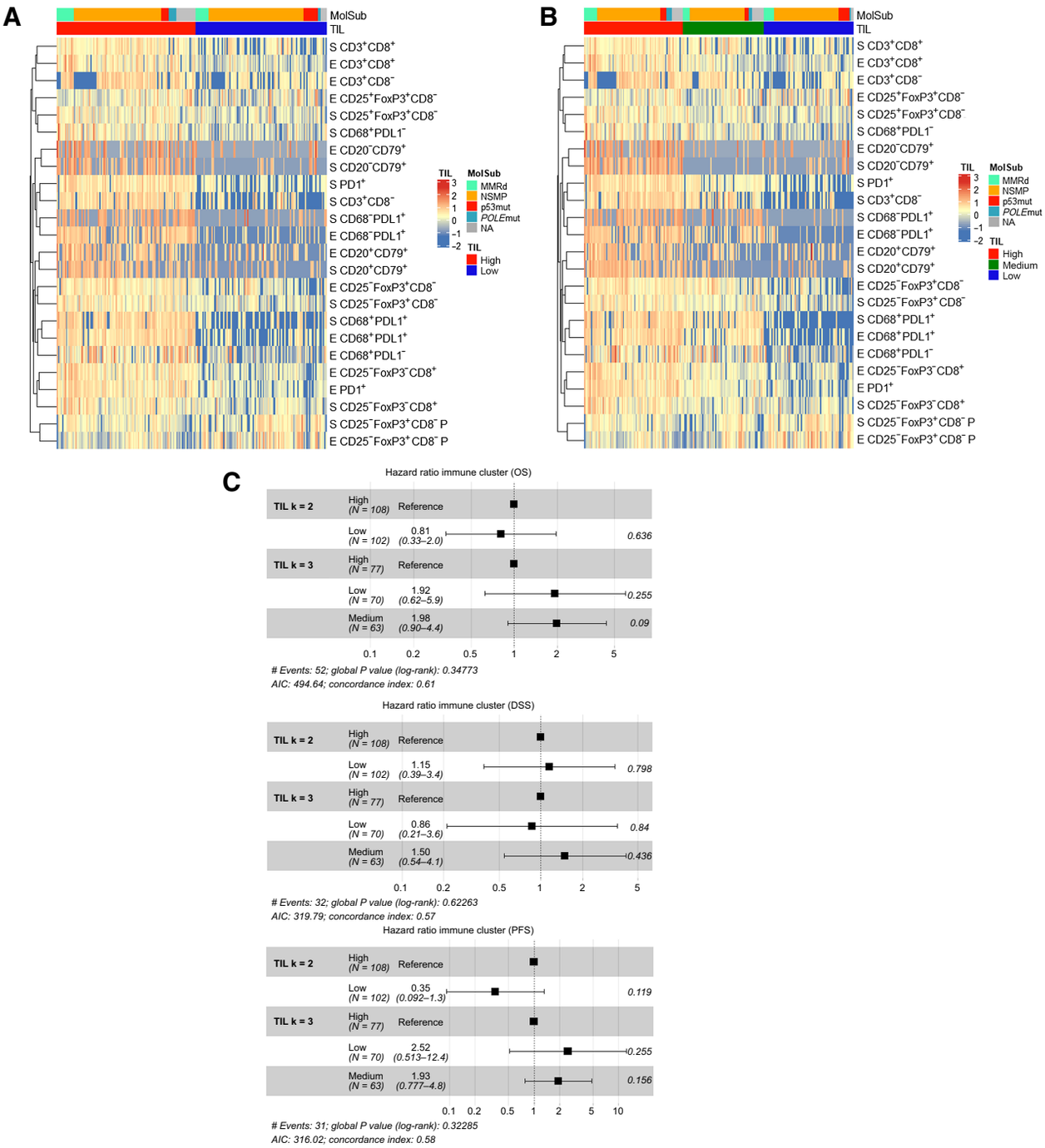

Figure 3.
Cluster analysis of TIL patterns for the optimal cluster solution k = 2 (**A**) and cluster alternative k = 3 (**B**). TIL_{high} tumors showed significantly higher densities in both T-cell lineage TIL subsets. **C,** Forest plot showing the individual HRs of both cluster solutions in regards to OS, DSS, and PFS.

analyses were carried out based on this. Within this, TIL_{high} was dominated by regulatory ($CD25^+/FoxP3^+$) and cytotoxic T ($CD3^+/CD8^+$ and $CD25^{L-}/FoxP3^-/CD8^+$) cells. The TIL_{medium} cluster also had high levels of T cells ($CD3^+$ populations) and macrophages ($CD68^+$ populations) and modest levels of intraepithelial $CD68^-/PD\text{-}L1^+$ cells but negligible levels of B-lineage cells ($CD20^+$ and/or $CD79a^+$). Consequently, we deemed this the $TIL_{B\ minus}$ cluster. Finally, the TIL_{low} cluster had a paucity of T cells, B cells, and PD-1^+ and PD-$L1^+$ populations and was notably devoid of macrophages ($CD68^+$; **Fig. 3B**). Intriguingly, the TIL_{low} cluster was significantly enriched for $FoxP3^+$

tumor cells ($CD25^{L-}$/$FoxP3^{+}$/$CD8^{-}$/$PanCK^{+}$) compared with TIL_{high}/$TIL_{B\ minus}$ combined ($P < 0.001$), whereas no such differences were found between TIL_{high} and $TIL_{B\ minus}$ tumors ($P = 0.11$). However, the k = 3 immune clusters also did not show distinct consistent survival outcomes for ENOC ($P > 0.1$).

Immune cells show prognostic significance in high-stage ENOC

ENOC typically presents at lower stage, thus we stratified analysis for low (FIGO I/II) and high (FIGO III/IV) stage. Immune clusters showed no prognostic effect in low-stage ENOC ($P > 0.1$; **Table 2A**). In high-stage ENOC, immune cluster groups showed a significant difference in OS ($HR_{B\ minus}$, 4.91; 95% CI, 1.58–15.3; $P < 0.05$), and a trend in PFS ($HR_{B\ minus}$, 3.57; 95% CI, 1.13–11.3; $P = 0.066$; **Table 2A**). In multivariable analysis, adjusting for clinicopathologic and molecular parameters (age, residual disease, grade, treatment, molecular subtype, and ARID1A status), high-stage $TIL_{B\ minus}$ cases did worse than TIL_{high} and TIL_{low} (HR_{high}, 0.19; 95% CI, 0.02–2.12; $HR_{B\ minus}$, 3.23; 95% CI, 0.52–23.0—reference TIL_{low}, respectively, both $P < 0.05$; data not shown).

Compartment-specific immune infiltration is dependent on subtype

We saw significant differences in immune cell density between subtypes in the epithelial compartment for cytotoxic T-cell populations ($CD3^{+}$/$CD8^{+}$ $P = 0.043$; and $CD25^{L-}$/$FoxP3^{-}$/$CD8^{+}$ $P < 0.001$; Supplementary Table S2), $FoxP3^{+}$ cells ($CD25^{L-}$/$FoxP3^{+}$/$CD8^{-}$ $P = 0.013$), PD-1^{+} cells ($P = 0.005$), and $CD68^{-}$/PD-$L1^{+}$ cells ($P = 0.011$). While these differences were generally driven by lower fraction of observed expression (52%–88% of detected expression) and lower infiltration (density values) in the p53abn subtype, $CD68^{-}$/PD-$L1^{+}$ cells also had low density in the NSMP subtype. The $CD25^{L-}$/$FoxP3^{-}$/$CD8^{+}$ population was the only one with subtype differences in both epithelial ($P < 0.001$) and stromal compartments ($P = 0.043$), dominantly driven by low density in p53abn (log-transformed values of −2.7 and 2.2, respectively). Stroma only infiltration was different across subtypes for $CD3^{+}$/$CD8^{-}$ cells ($P = 0.048$) with the highest densities in the NSMP group (Supplementary Table S2). $CD68^{+}$/PD-$L1^{-}$ macrophage densities also varied by subtype in the stromal

Table 2. Summary of *P* values obtained during Kaplan–Meier survival analysis in regard to TILs and subtypes.

A	Log-rank test *P*		OS HR (95% CI)	OS *P*	DSS HR (95% CI)	DSS *P*	PFS HR (95% CI)	PFS *P*
	Low stage							
	Immune k = 3	Low	1.78 (0.72–4.41)	0.429	1.03 (0.26–4.14)	0.892	1.19 (0.36–3.91)	0.886
	ref: high	B minus	1.24 (0.48–3.20)		1.33 (0.36–4.96)		0.88 (0.24–3.26)	
	Molecular subtype	p53abn	0.58 (0.14–2.45)	0.148	1.03 (0.21–5.12)	<**0.05**	1.13 (0.23–5.59)	0.07
	ref: MMRd	NSMP	0.40 (0.15–1.11)		0.21 (0.05–0.88)		0.31 (0.08–1.17)	
		*POLE*mut	0.00 (0.0–0.0)		0.0 (0.0–0.0)		0.0 (0.0–0.0)	
	High stage							
	Immune k = 3	Low	2.86 (0.89–9.39)	<**0.05**	2.43 (0.70–8.43)	0.134	1.38 (0.35–5.53)	0.066
	ref: high	B minus	4.91 (1.58–15.3)		3.22 (0.92–11.3)		3.57 (1.13–11.3)	
	Molecular subtype	p53abn	5.65 (0.63–51.1)	0.191	5.22 (0.58–47.2)	0.282	2.13 (0.35–12.8)	0.631
	ref: MMRd	NSMP	5.3 (0.68–41.5)		3.75 (0.47–30.3)		2.02 (0.44–9.36)	
		*POLE*mut	—		—		—	

B	Log-rank test *P*	ref: high	OS HR (95% CI)	OS *P*	DSS HR (95% CI)	DSS *P*	PFS HR (95% CI)	PFS *P*
	Immune k = 3							
	MMRd	Low	2.09 (0.35–12.6)	0.707	1.37 (0.19–9.85)	0.614	1.58 (0.22–11.3)	0.898
		B minus	1.29 (0.11–14.7)		0.0 (0.0–0.0)		1.16 (0.10–12.9)	
	p53abn	Low	0.37 (0.07–1.87)	0.362	0.37 (0.07–1.87)	0.362	0.41 (0.07–2.50)	0.338
		B minus	1.05 (0.17–6.38)		1.05 (0.17–6.38)		1.37 (0.19–9.83)	
	NSMP	Low	2.36 (0.82–6.8)	<**0.05**	0.97 (0.2–4.79)	<**0.05**	0.65 (0.18–2.29)	0.426
		B minus	3.64 (1.31–10.1)		4.03 (1.11–14.7)		1.44 (0.48–4.27)	

C	Low-stage ENOC							
	Log-rank test *P*	ref: high	OS HR (95% CI)	OS *P*	DSS HR (95% CI)	DSS *P*	PFS HR (95% CI)	PFS *P*
	Immune k = 3							
	MMRd	Low	1.87 (0.19–18.4)	0.857	1.34 (0.12–15.3)	0.647	1.3 (0.11–14.8)	0.548
		B minus	1.45 (0.08–26.2)		0.0 (0.0–0.0)		0.0 (0.0–0.0)	
	p53abn	Low	2.1*e8 (0.0–0.0)	0.674	2.1*e8 (0.0–0.0)	0.674	2.1*e8 (0.0–0.0)	0.664
		B minus	3.7*e8 (0.0–0.0)		3.7*e8 (0.0–0.0)		3.9*e8 (0.0–0.0)	
	NSMP	Low	1.83 (0.53–6.29)	0.62	0.0 (0.0–0.0)	0.184	0.63 (0.11–3.77)	0.804
		B minus	1.52 (0.41–5.67)		1.69 (0.28–10.1)		1.12 (0.23–5.57)	

Note: **A,** Effects of the immune cluster and molecular subtype on survival outcomes within ENOC. **B** and **C,** Survival analysis in regard to TIL clusters within the respective molecular subtype in all of ENOC (**B**) and only low-staged ENOC (**C**). Because of a lack of cases and events, analyses within the *POLE*mut subtype were inconclusive and therefore excluded.

compartment ($P = 0.004$) driven by high density in *POLE*mut/MMRd and marked lower density in p53abn. B-lymphocyte lineage populations including cells staining for CD20 and/or CD79a were the least prevalent populations with overall low densities observed across all subtypes. Although higher plasma cell density was seen in *POLE*mut/MMRd, and exceptionally low densities in p53abn, this was not significant (epithelial compartment $P = 0.099$; Supplementary Table S2).

Overlay of molecular subtype and immune infiltration clusters in ENOC

Because our previous EC study showed that molecular subtypes were superior to TIL patterns for prognostication (23), we reanalyzed ENOC cases including molecular subtype and immune cluster labels. In univariable analysis, immune clustering had no benefit, while prognostic value of the molecular subtype retained its significance in DSS and PFS ($P < 0.05$; Supplementary Table S4).

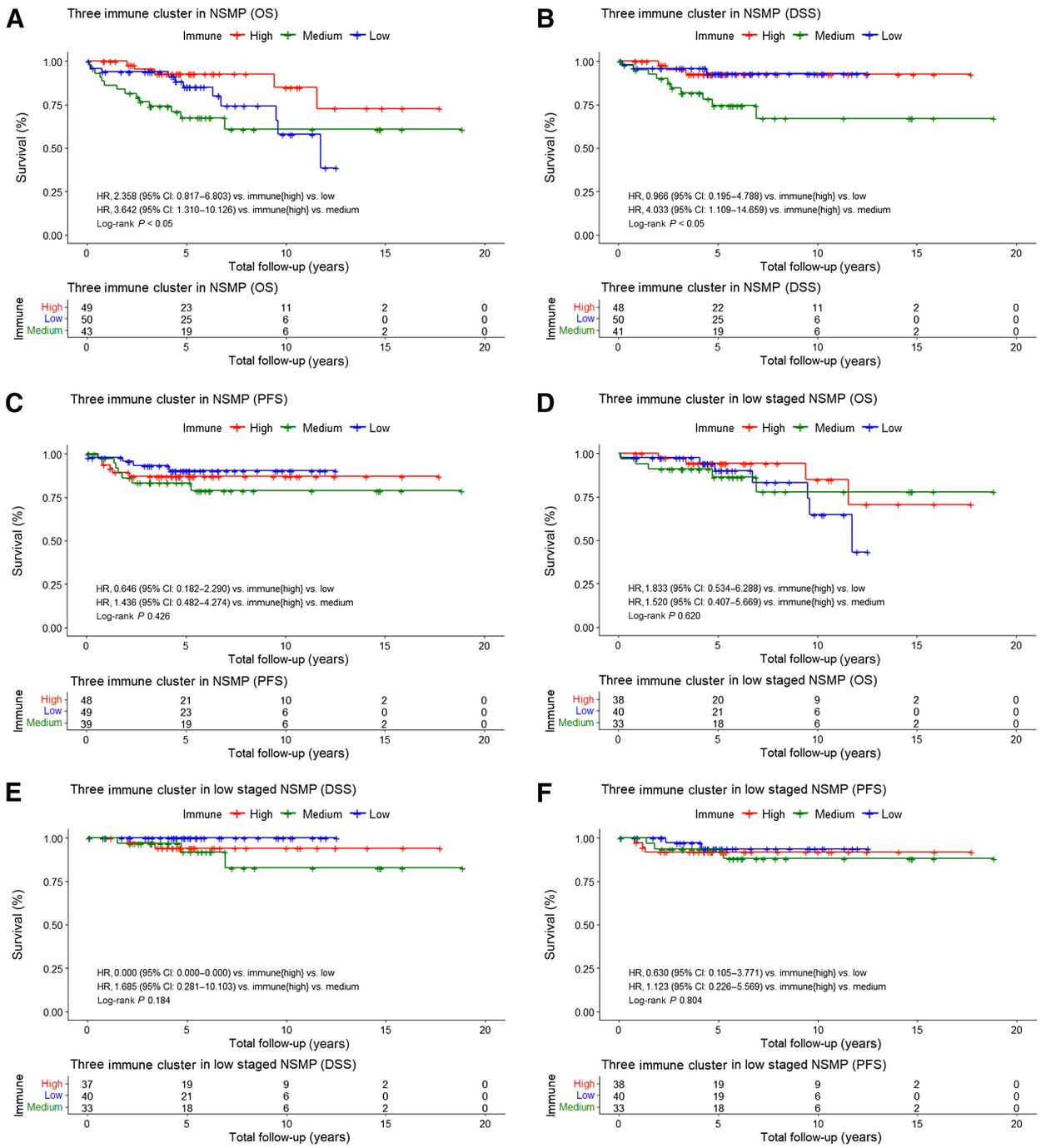

Figure 4.
Benefit of immune response in NSMP ENOC. Kaplan–Meier curves of OS, DSS, and PFS in regards to TIL pattern k = 3 in all NSMP (**A–C**), in low-stage NSMP (**D–F**),
(*Continued on the following page.*)

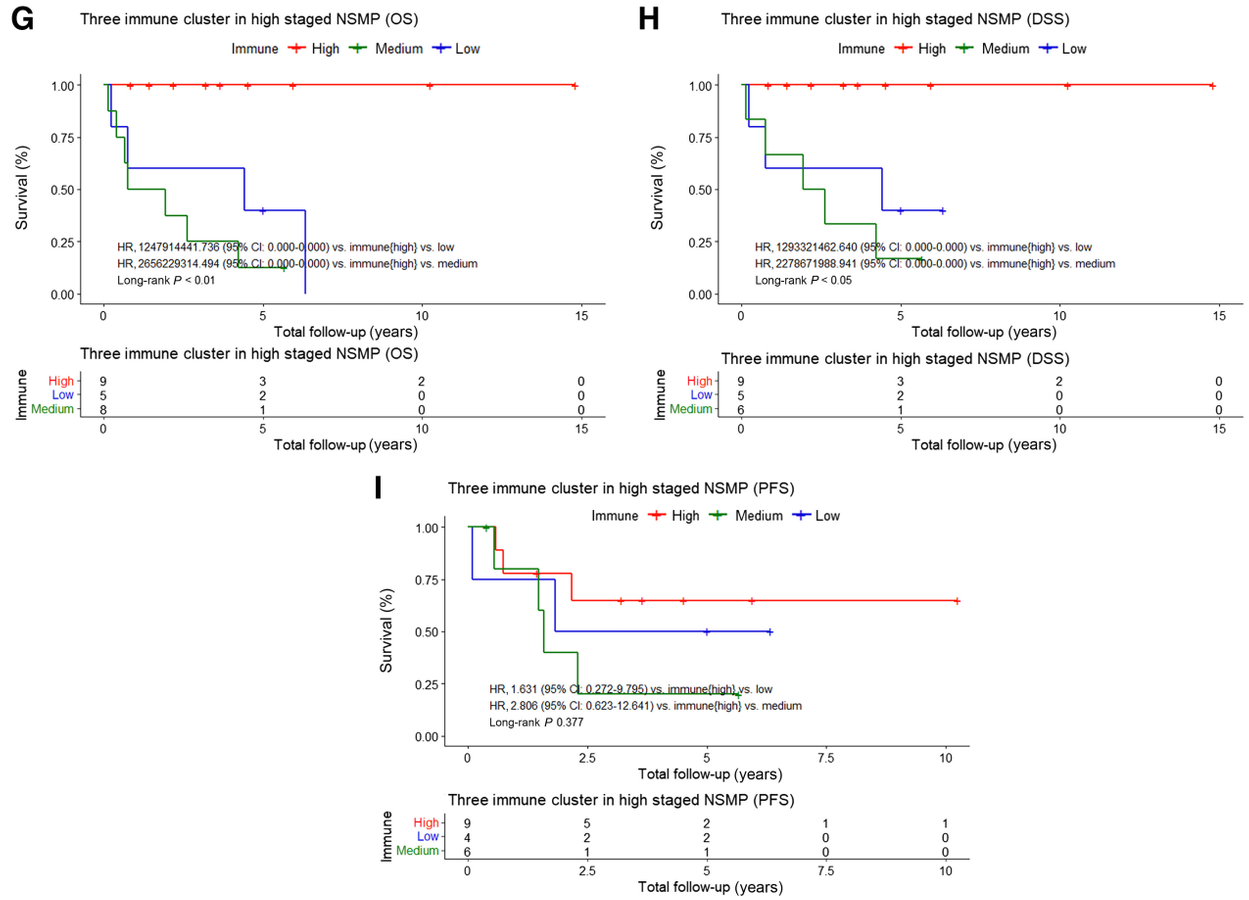

Figure 4.
(*Continued.*) and high-stage NSMP (**G–I**).

We next stratified the analysis by subtype. *POLE*mut ENOC cases ($n = 8$) were omitted from this analysis due to small numbers and a lack of death or progression events. In the NSMP subtype, the $TIL_{B\ minus}$ cluster performed significantly worse for OS and DSS than the TIL_{high} and TIL_{low} clusters (OS: HR, 3.64; 95% CI, 1.31–10.1; DSS: HR, 4.03; 95% CI, 1.11–14.7; both $P < 0.05$; **Table 2B**; **Fig. 4**).

We repeated this analysis further stratifying cases by low and high stage. In the MMRd and p53abn subtype, no differences were seen between TIL clusters in low-stage cases; analyses were not performed on high-stage cases due to insufficient sample size numbers (**Table 2C**). Amongst high-stage ENOC the more prevalent NSMP group showed striking differences for the k = 3 solution in OS and DSS (HR > 20; 95% CI, 0.0–0.0; both $P < 0.05$; **Fig. 4**). The three cluster groups remained significant for multivariable analysis amongst NSMP for OS and DSS when considering all stages of NSMP (both $HR_{B\ minus} > 1.4$; $P \leq 0.01$), but not for high-stage restricted DSS analysis (Supplementary Table S5).

Within the NSMP ENOC, the $TIL_{B\ minus}$ cluster was characterized by an absence of plasma and B cells ($CD20^{-/+}/CD79a^{+}$), which was also seen with the TIL_{low} cluster ($P > 0.3$, data not shown). A retention of macrophages ($CD68^{+}$), especially PD-L1^{-} macrophages, and cytotoxic T cells ($CD3^{+}/CD8^{+}$ and $CD25^{-}/FoxP3^{-}/CD8^{+}$) similar to the TIL_{high} cluster was seen. Furthermore, intermediate to high levels of PD-1^{+} cells and regulatory T cells ($CD25^{+}/FoxP3^{+}/CD8^{-}$ and $CD25^{-}/FoxP3^{+}/CD8^{-}$ respectively) were observed in this NSMP $TIL_{B\ minus}$ group. Surprisingly, the highest mean density of $CD3^{+}/CD8^{-}$ (helper) T cells was recorded in this subcohort (log transformed mean: 0.35 in $TIL_{B\ minus}$ vs. −0.67 in TIL_{high} and −4.6 in TIL_{low}). This was also observed in high-stage NSMP $TIL_{B\ minus}$ cases, where additionally not even one case with infiltrating B cell was recorded.

Investigating correlations with other ENOC prognostic biomarkers, we did not see associations between the $TIL_{B\ minus}$ cluster and any of progesterone receptor (PR), estrogen receptor (ER), or β-catenin positivity (all $P > 0.1$; Supplementary Fig. S3). However, we did note that a larger proportion of NSMP $TIL_{B\ minus}$ cases had PR-positive staining compared with the other two clusters (88.4% vs. 83.7/74% in $TIL_{high/low}$; $P = 0.188$; Supplementary Fig. S3).

Similarity between ovarian and endometrial endometrioid tumors

With data generally similar to trends observed in endometrial cancer we reexamined EEC from our previous dataset (23) to compare and contrast with ENOC. The EEC subtype distribution and resulting outcomes were generally similar to the full endometrial cancer

cohort (Supplementary Fig. S4B–S4D; ref. 23). The majority of EEC cases (55.6%) were NSMP, 25.8% MMRd, 10.8% *POLE*mut, and 7.8% p53abn. A full side-by-side comparison of the considered immune cell populations could not be done since partially different IHC/IF panels were used between the two data sets (e.g., no assessment of FoxP3 and PanCK co-staining cells in EEC). Like ENOC, immune clustering in either k = 2 or k = 3 did not result in significant survival benefit among the full EEC cohort (OS, DSS, PFS $P > 0.5$; Supplementary Fig. S4). In contrast to ENOC, in the NSMP EEC subcohort we saw no survival advantage with the k = 3 immune cluster solution ($P > 0.05$; Supplementary Fig. S4E–S4G).

Discussion

In this study, we evaluated the iTME across the four molecular subtypes of endometrioid ovarian carcinoma. Immune cell infiltrates showed three distinct patterns: a "TIL_{low}" or cold cluster, a "TIL_{high}" or hot cluster with a combined T- and B-cell response, and a "$TIL_{B\ minus}$" cluster that was distinguished by T cells with negligible B and plasma cells. TIL levels were higher in high-stage ENOC. Across the overall ENOC cohort, molecular subtyping presented superior prognostic significance compared to immune cell infiltrates alone. Nonetheless, after molecular subtype stratification, immune infiltrates showed prognostic value in the NSMP subtype, with the $TIL_{B\ minus}$ cluster showing significantly worse survival than the TIL_{high} and TIL_{low} clusters.

We examined a cohort of 210 ENOC which were previously characterized by pathology review and IHC-based confirmation of the histotype (8). A total of 190 cases had full molecular subtype annotation; the prevalence of these subtypes was similar to other reports, as were the overall clinicopathological features (age, stage, grade, residual disease) and ARID1A loss enriched in the MMRd subtype (7, 8, 11). On average, when evaluating the different compartment restricted immune cell populations, an association with outcome benefits was seen across the full ENOC cohort. High level of cytotoxic $CD8^+$ ($CD25^{L-}$/$FoxP3^-$/$CD8^+$) T cells or plasma cells ($CD20^+$/$CD79a^+$) in the stroma were linked to better survival outcomes, consistent with HGSOC (50, 51). However, given a relatively weak HR for this observation, including all ENOC, it is likely a diluted effect from the majority NSMP subset. It should also be noted our cohort was smaller than the previous reports and the described effect was subtle in ENOC (6, 7).

Clustering of the immune cell densities revealed three dominant immune phenotypes (TIL_{high}, $TIL_{B\ minus}$, and TIL_{low}); however, examination of ENOC as a whole suggested these phenotypes had no significant outcome benefits. High-stage ENOC outcomes appeared to be more influenced by immune infiltration and clusters with generally higher levels of TILs had better OS with supporting trends in DSS and/or PFS, although this may be confounded with molecular subtype (7, 8). While a general trend of high-moderate-low overall immune infiltration could be observed across these clusters, $FoxP3^+$ tumor cells showed a distinct pattern. FoxP3 is typically used as a marker of regulatory T cells; however, our and others' analyses indicate FoxP3 can also be expressed by tumor cells (52, 53). Although it has been suggested that epithelial FoxP3 expression influences carcinogenesis and outcome in other cancers (54, 55), no effect on outcomes was observed here in ENOC. Further studies into the nature of $FoxP3^+$ tumor cells may still be warranted to better describe this biologically distinct group with otherwise low levels of immune infiltration.

Molecular subtype influenced the immune cell density across both the epithelial and stromal compartments. Consistent with findings in endometrial cancer (23), molecular subtypes with higher mutational burden tended to have a greater level of immune cell infiltration. That said, a wide range of immune cell densities was visible within each subtype, and no immune cluster group was entirely confined to any one molecular subtype. *POLE*mut and MMRd subgroups were enriched for TIL_{high} tumors and had the highest levels of intraepithelial $PD\text{-}L1^+$ cells. Consistent with this, PD-L1 positivity has been associated with improved outcomes in HGSOC and endometrial cancer (56, 57). High infiltration of $PD\text{-}1^+$ cells was also observed across epithelial compartments of all molecular subtypes, except for p53abn cases. In p53abn ENOC an absence and low density of cytotoxic T ($CD8^+$) cells was recorded in stromal and epithelial compartments. In fact, only a few $CD3^+$/$CD8^-$ lymphocytes were detected in p53abn stroma, while they were most prevalent in the stromal compartment of NSMP tumors (p53 wild-type). This may be consistent with recent reports suggesting that perturbed p53 leads to an immune suppressive and tumor promoting environment, manifested as reduced cytotoxic cells and increased inhibitory myeloid cells (58, 59).

Overlaying molecular subtype and immune density clustering did not add additional prognostic value over molecular subtype alone. However, restricted analysis of NSMP ENOC suggested the $TIL_{B\ minus}$ cluster performed significantly worse than others. Likewise, superior performance of TIL_{high} tumors was most evident in high-stage NSMP, however, this observation was based on a small number of cases ($n = 20$) and has to be seen in more of an exploratory sense.

The $TIL_{B\ minus}$ NSMP cluster was characterized by relatively high levels of $PD\text{-}L1^-$ macrophages, cytotoxic T cells, $CD8^-$ (helper) T cells and FoxP3-expressing (regulatory) T cells in epithelial compartments. Indeed, the levels of those cell types in $TIL_{B\ minus}$ were not significantly different from the TIL_{high} cluster; however, it remains unknown whether these immune infiltrates might be exhausted or dysfunctional within their iTME. Likewise, $TIL_{B\ minus}$ tumors almost entirely lacked B or plasma cells. In other cancers, high levels of B cells, especially in tertiary lymphoid structures, can modulate the overall iTME and positively influence outcome and prognosis (51, 60). One could additionally speculate that the lack of B cells in $TIL_{B\ minus}$ tumors shifts T cells towards a more suppressive phenotype, which aligns with accumulating evidence that B-lineage cells have a net positive influence on antitumor immunity (61). Because our IHC/IF data were based on TMAs rather than whole tissue sections, it is possible that we have underestimated B and plasma cell responses involving tertiary lymphoid structures. Nonetheless, high levels of cytotoxic and Th cells $PD\text{-}L1^+$ macrophages, suggest PD-1/PD-L1-directed ICI therapy may be effective (62). Similarly, cases with a high level of regulatory T cells may also benefit from ICIs as activating these populations has been shown to recruit cancer antigen–specific effector cells and potentiate immune therapy responses (63). These observations should be correlated to data from ICI trials including ENOC and/or in functional, immune-competent, models.

This is among the first reports of TIL_{low} (ovarian) tumors being associated with more favorable prognosis than $TIL_{B\ minus}$ tumors, which exhibit a medium level of immune infiltration. This could be attributed to a low-stage cohort, typical of ENOC. Indeed, while immune cell cluster distributions were similar in stage I and II cases, an enrichment of TIL_{high} tumors was seen stage III and IV cases. However, we do want to point out that an effect overestimation based on small sample size in the sub analyses may be present.

Given the known similarity between endometrial cancer, and especially EEC, with ENOC we were unsurprised to find similar trends related to immune cell infiltration (23). However, as there were differences in the immune cell panels examined between endometrial cancer and ENOC cohorts some subtlety between the uterine versus ovarian environments may have been missed. In fact, we were not able to recapitulate a poor-outcome $TIL_{B\ minus}$ cluster in EEC and it is unclear if this is a result of ovarian-specific microenvironment or panel differences between studies. Nonetheless our data are still supportive of future ENOC trials being combined with endometrial cancer /EEC. This may be particularly beneficial for NSMP tumors which are not well characterized in either the ovarian or uterine presentation. While NSMP tumors are proportionally less common among endometrial cancer/EEC compared with ENOC, endometrial cancer overall is a much more common cancer. Large-scale studies of endometrial cancer suggest there are a number of mutations prevalent across NSMP tumors, however, those are less uniform than the other subtypes such that NSMP is generally regarded as a subtype by omission: lacking *POLE* mutation, MMRd/MSI, and high levels of DNA copy-number alterations (p53-abnormality). The same is true for their ENOC counterparts, and both may benefit from further stratification. The value of biomarkers that add prognostic (and potentially predictive) information to NSMP tumors is high. Our study suggests immune infiltration may be a valid and independent stratification mechanism in NSMP. However, as the usage of multiplex IHC and/or IF is limited in current clinical practice, simpler signatures and surrogate biomarker investigations are still needed to make these findings clinically applicable.

In ENOC and endometrial cancer, the presence of hormone receptors, especially PR, has been associated with favorable outcome (45, 64). Indeed investigation of hormone-based therapies is a prime candidate for NSMP endometrial cancer trials (65). In our NSMP ENOC cohorts, both PR and ER showed prognostic significance. However, no correlation was seen between the immune clusters and positivity for either hormone receptor. This suggests that the prognostic effect of the immune cluster in NSMP ENOC may be independent of PR/ER status. Our study is the first multifaceted iTME evaluation in ENOC in the context of molecular subtypes. This highlights the value of considering molecular subtype stratification in prognostication prior to targeted therapeutic considerations or other stratification. Consequently, for prognostication of NSMP cases, we suggest a tiered stratification system first by molecular subtype and second by immune response may be beneficial. Our data also propose that the NSMP subtype warrants consideration for immunotherapy clinical trials.

Authors' Disclosures

K. Heinze reports grants from Deutsche Forschungsgesellschaft during the conduct of the study. S. Fereday reports grants from NHMRC during the conduct of the study, as well as grants from AstraZeneca outside the submitted work. D.W. Garsed reports grants from National Health and Medical Research Council of Australia (NHMRC), U.S. Army Medical Research and Materiel Command Ovarian Cancer Research Program, and Victorian Cancer Agency during the conduct of the study. P. Harter reports grants, personal fees, and non-financial support from AstraZeneca; grants and personal fees from GSK, MSD, Mersana, Immunogen, and Novartis; personal fees from Amgen, Sotio, Stryker, Zai Lab, Eisai, Exscientia, and Miltenyi Biotec; and grants from Roche, Clovis, Genmab, and Seagen outside the submitted work. F. Heitz reports personal fees from NovoCure, PharmaMar, Tesaro, GSK, and Clovis; personal fees and non-financial support from AstraZeneca and Roche; and non-financial support from Amedes outside the submitted work. A. DeFazio reports grants from U.S. Army Medical Research and Materiel Command Ovarian Cancer Research Program during the conduct of the study, as well as grants from AstraZeneca outside the submitted work. D.D.L. Bowtell reports grants from Genentech, Roche, and AstraZeneca, as well as personal fees from Exo Therapeutics outside the submitted work. M. Pike was supported in part through the NIH/NCI Support Grant P30 CA008748 (principal investigator: S.M. Vickers) to Memorial Sloan Kettering Cancer Center. C.L. Pearce reports grants from NIH and grants from DoD during the conduct of the study. A. Staebler reports personal fees from Thermo Fisher Scientific and AstraZeneca outside the submitted work. S. Kommoss reports grants and personal fees from GSK, as well as personal fees from MSD, AstraZeneca, and Eisai outside the submitted work. B.H. Nelson reports grants from U.S. DoD during the conduct of the study. M.S. Anglesio reports grants from Canadian Institutes of Health Research, Janet D. Cottrelle Foundation, and Michael Smith Health Research BC during the conduct of the study. No disclosures were reported by the other authors.

Disclaimer

The contents of the published material are solely the responsibility of the authors and do not reflect the views of NHMRC.

Authors' Contributions

K. Heinze: Conceptualization, validation, investigation, writing–original draft, specimen identification. **E.S. Cairns:** Sample processing. **S. Thornton:** Sample processing. **B. Harris:** Sample processing. **K. Milne:** Methodology, sample processing. **M. Grube:** Resources, specimen identification. **C. Meyer:** Specimen identification. **A.N. Karnezis:** Methodology. **S. Fereday:** Methodology. **D.W. Garsed:** Methodology. **S.C.Y. Leung:** Resources. **D.S. Chiu:** Resources. **M. Moubarak:** Resources. **P. Harter:** Resources. **F. Heitz:** Resources. **J.N. McAlpine:** Resources, methodology. **A. DeFazio:** Methodology. **D.D.L. Bowtell:** Methodology. **E.L. Goode:** Methodology. **M. Pike:** Methodology. **S.J. Ramus:** Methodology, specimen identification. **C.L. Pearce:** Methodology, specimen identification. **A. Staebler:** Resources, specimen identification. **M. Köbel:** Pathology and IHC review. **S. Kommoss:** Resources, specimen identification. **A. Talhouk:** Investigation. **B.H. Nelson:** Conceptualization, investigation, methodology. **M.S. Anglesio:** Conceptualization, investigation, methodology, specimen identification.

Acknowledgments

We thank all the study participants who contributed to this study and all the researchers, clinicians, and technical and administrative staff who have made this work possible. We further acknowledge the following financial support: This research was funded in part by the Janet D. Cottrelle Foundation and the Canadian Institutes of Health Research (Early Career Investigator Grant, to M.S. Anglesio). K. Heinze is funded through a research scholarship by the Deutsche Forschungsgesellschaft (HE 8699/1–1). A. Talhouk is funded through a Michael Smith Foundation for Health Research Scholar Award. M.S. Anglesio is funded through a Michael Smith Foundation for Health Research Scholar Award and the Janet D. Cottrelle Foundation Scholars program managed by the BC Cancer Foundation. BC's Gynecological Cancer Research team (OVCARE) receives support through the BC Cancer Foundation and the VGH & UBC Hospital Foundation. S.J. Ramus and D.W. Garsed are supported by National Health and Medical Research Council of Australia (NHMRC) grant APP2009840 (to S.J. Ramus) and grant 1186505 (to D.W. Garsed). This work was supported by the U.S. Army Medical Research and Materiel Command Ovarian Cancer Research Program (award no. W81XWH-16–2-0010). D.W. Garsed is further supported by the U.S. Army Medical Research and Materiel Command Ovarian Cancer Research Program (award no. W81XWH-21–1-0401) and the Victorian Cancer Agency (MCRF22018). E.L. Goode is supported through the following grants: P30-CA015083, P50-CA136939, R01-CA248288. M. Pike was supported in part through the NIH/NCI Support Grant P30 CA008748 (principal investigator: S.M. Vickers) to Memorial Sloan Kettering Cancer Center.

The publication costs of this article were defrayed in part by the payment of publication fees. Therefore, and solely to indicate this fact, this article is hereby marked "advertisement" in accordance with 18 USC section 1734.

Note

Supplementary data for this article are available at Clinical Cancer Research Online (http://clincancerres.aacrjournals.org/).

Received February 15, 2023; revised April 14, 2023; accepted June 14, 2023; published first June 20, 2023.

References

1. Kobel M, Kalloger SE, Lee S, Duggan MA, Kelemen LE, Prentice L, et al. Biomarker-based ovarian carcinoma typing: a histologic investigation in the ovarian tumor tissue analysis consortium. Cancer Epidemiol Biomarkers Prev 2013;22:1677–86.
2. Kobel M, Kalloger SE, Santos JL, Huntsman DG, Gilks CB, Swenerton KD. Tumor type and substage predict survival in stage I and II ovarian carcinoma: insights and implications. Gynecol Oncol 2010;116:50–6.
3. Kobel M, Bak J, Bertelsen BI, Carpen O, Grove A, Hansen ES, et al. Ovarian carcinoma histotype determination is highly reproducible, and is improved through the use of immunohistochemistry. Histopathology 2014;64:1004–13.
4. Vaughan S, Coward JI, Bast RC Jr, Berchuck A, Berek JS, Brenton JD, et al. Rethinking ovarian cancer: recommendations for improving outcomes. Nat Rev Cancer 2011;11:719–25.
5. Kalloger SE, Kobel M, Leung S, Mehl E, Gao D, Marcon KM, et al. Calculator for ovarian carcinoma subtype prediction. Mod Pathol 2011;24:512–21.
6. Ovarian Tumor Tissue Analysis (OTTA) Consortium, Goode EL, Block MS, Kalli KR, Vierkant RA, Chen W, et al. Dose-response association of CD8+ tumor-infiltrating lymphocytes and survival time in high-grade serous ovarian cancer. JAMA Oncol 2017;3:e173290.
7. Heinze K, Nazeran TM, Lee S, Kramer P, Cairns ES, Chiu DS, et al. Validated biomarker assays confirm that ARID1A loss is confounded with MMR deficiency, CD8(+) TIL infiltration, and provides no independent prognostic value in endometriosis-associated ovarian carcinomas. J Pathol 2022;256:388–401.
8. Kramer P, Talhouk A, Brett MA, Chiu DS, Cairns ES, Scheunhage DA, et al. Endometrial cancer molecular risk stratification is equally prognostic for endometrioid ovarian carcinoma. Clin Cancer Res 2020;26:5400–10.
9. Schultheis AM, Ng CK, De Filippo MR, Piscuoglio S, Macedo GS, Gatius S, et al. Massively parallel sequencing-based clonality analysis of synchronous endometrioid endometrial and ovarian carcinomas. J Natl Cancer Inst 2016;108:djv427.
10. Anglesio MS, Wang YK, Maassen M, Horlings HM, Bashashati A, Senz J, et al. Synchronous endometrial and ovarian carcinomas: evidence of clonality. J Natl Cancer Inst 2016;108:djv428.
11. Leskela S, Romero I, Rosa-Rosa JM, Caniego-Casas T, Cristobal E, Perez-Mies B, et al. Molecular heterogeneity of endometrioid ovarian carcinoma: an analysis of 166 cases using the endometrial cancer subrogate molecular classification. Am J Surg Pathol 2020;44:982–90.
12. Duska LR, Kohn EC. The new classifications of ovarian, fallopian tube, and primary peritoneal cancer and their clinical implications. Ann Oncol 2017;28:viii8–viii12.
13. Machida H, Matsuo K, Yamagami W, Ebina Y, Kobayashi Y, Tabata T, et al. Trends and characteristics of epithelial ovarian cancer in Japan between 2002 and 2015: A JSGO-JSOG joint study. Gynecol Oncol 2019;153:589–96.
14. Alvarez RD, Karlan BY, Strauss JF. "Ovarian cancers: evolving paradigms in research and care": report from the Institute of Medicine. Gynecol Oncol 2016;141:413–5.
15. Anglesio MS, Yong PJ. Endometriosis-associated ovarian cancers. Clin Obstet Gynecol 2017;60:711–27.
16. Wendel JRH, Wang X, Hawkins SM. The endometriotic tumor microenvironment in ovarian cancer. Cancers (Basel) 2018;10:261.
17. Leon-Castillo A, Britton H, McConechy MK, McAlpine JN, Nout R, Kommoss S, et al. Interpretation of somatic POLE mutations in endometrial carcinoma. J Pathol 2020;250:323–35.
18. Cancer Genome Atlas Research Network, Kandoth C, Schultz N, Cherniack AD, Akbani R, Liu Y, et al. Integrated genomic characterization of endometrial carcinoma. Nature 2013;497:67–73.
19. McAlpine J, Leon-Castillo A, Bosse T. The rise of a novel classification system for endometrial carcinoma; integration of molecular subclasses. J Pathol 2018;244:538–49.
20. Talhouk A, McConechy MK, Leung S, Li-Chang HH, Kwon JS, Melnyk N, et al. A clinically applicable molecular-based classification for endometrial cancers. Br J Cancer 2015;113:299–310.
21. Talhouk A, McConechy MK, Leung S, Yang W, Lum A, Senz J, et al. Confirmation of ProMisE: A simple, genomics-based clinical classifier for endometrial cancer. Cancer 2017;123:802–13.
22. Kommoss S, McConechy MK, Kommoss F, Leung S, Bunz A, Magrill J, et al. Final validation of the ProMisE molecular classifier for endometrial carcinoma in a large population-based case series. Ann Oncol 2018;29:1180–8.
23. Talhouk A, Derocher H, Schmidt P, Leung S, Milne K, Gilks CB, et al. Molecular subtype not immune response drives outcomes in endometrial carcinoma. Clin Cancer Res 2019;25:2537–48.
24. Parra-Herran C, Lerner-Ellis J, Xu B, Khalouei S, Bassiouny D, Cesari M, et al. Molecular-based classification algorithm for endometrial carcinoma categorizes ovarian endometrioid carcinoma into prognostically significant groups. Mod Pathol 2017;30:1748–59.
25. Cybulska P, Paula ADC, Tseng J, Leitao MM Jr., Bashashati A, Huntsman DG, et al. Molecular profiling and molecular classification of endometrioid ovarian carcinomas. Gynecol Oncol 2019;154:516–23.
26. Duan Q, Zhang H, Zheng J, Zhang L. Turning cold into hot: firing up the tumor microenvironment. Trends Cancer 2020;6:605–18.
27. Brown SD, Warren RL, Gibb EA, Martin SD, Spinelli JJ, Nelson BH, et al. Neoantigens predicted by tumor genome meta-analysis correlate with increased patient survival. Genome Res 2014;24:743–50.
28. Ghisoni E, Imbimbo M, Zimmermann S, Valabrega G. Ovarian cancer immunotherapy: turning up the heat. Int J Mol Sci 2019;20:2927.
29. Topalian SL, Hodi FS, Brahmer JR, Gettinger SN, Smith DC, McDermott DF, et al. Safety, activity, and immune correlates of anti-PD-1 antibody in cancer. N Engl J Med 2012;366:2443–54.
30. Kim JY, Kronbichler A, Eisenhut M, Hong SH, van der Vliet HJ, Kang J, et al. Tumor mutational burden and efficacy of immune checkpoint inhibitors: a systematic review and meta-analysis. Cancers (Basel) 2019;11:1798.
31. Gooden MJ, de Bock GH, Leffers N, Daemen T, Nijman HW. The prognostic influence of tumour-infiltrating lymphocytes in cancer: a systematic review with meta-analysis. Br J Cancer 2011;105:93–103.
32. Zhang L, Conejo-Garcia JR, Katsaros D, Gimotty PA, Massobrio M, Regnani G, et al. Intratumoral T cells, recurrence, and survival in epithelial ovarian cancer. N Engl J Med 2003;348:203–13.
33. Briggs S, Tomlinson I. Germline and somatic polymerase epsilon and delta mutations define a new class of hypermutated colorectal and endometrial cancers. J Pathol 2013;230:148–53.
34. DiGuardo MA, Davila JI, Jackson RA, Nair AA, Fadra N, Minn KT, et al. RNA-seq reveals differences in expressed tumor mutation burden in colorectal and endometrial cancers with and without defective DNA-mismatch repair. J Mol Diagn 2021;23:555–64.
35. McConechy MK, Talhouk A, Leung S, Chiu D, Yang W, Senz J, et al. Endometrial carcinomas with POLE exonuclease domain mutations have a favorable prognosis. Clin Cancer Res 2016;22:2865–73.
36. Howitt BE, Shukla SA, Sholl LM, Ritterhouse LL, Watkins JC, Rodig S, et al. Association of polymerase e-mutated and microsatellite-instable endometrial cancers with neoantigen load, number of tumor-infiltrating lymphocytes, and expression of PD-1 and PD-L1. JAMA Oncol 2015;1:1319–23.
37. Bellone S, Centritto F, Black J, Schwab C, English D, Cocco E, et al. Polymerase epsilon (POLE) ultra-mutated tumors induce robust tumor-specific CD4+ T cell responses in endometrial cancer patients. Gynecol Oncol 2015;138:11–7.
38. Colombo N, Sessa C, du Bois A, Ledermann J, McCluggage WG, McNeish I, et al. ESMO-ESGO consensus conference recommendations on ovarian cancer: pathology and molecular biology, early and advanced stages, borderline tumours and recurrent disease†. Ann Oncol 2019;30:672–705.
39. Oseledchyk A, Leitao MM Jr, Konner J, O'Cearbhaill RE, Zamarin D, Sonoda Y, et al. Adjuvant chemotherapy in patients with stage I endometrioid or clear cell ovarian cancer in the platinum era: a surveillance, epidemiology, and end results cohort study, 2000–2013. Ann Oncol 2017;28:2985–93.
40. Concin N, Matias-Guiu X, Vergote I, Cibula D, Mirza MR, Marnitz S, et al. ESGO/ESTRO/ESP guidelines for the management of patients with endometrial carcinoma. Int J Gynecol Cancer 2021;31:12–39.
41. Chen S, Li Y, Qian L, Deng S, Liu L, Xiao W, et al. A review of the clinical characteristics and novel molecular subtypes of endometrioid ovarian cancer. Front Oncol 2021;11:668151.
42. Kurman RJ, Shih IM. Molecular pathogenesis and extraovarian origin of epithelial ovarian cancer–shifting the paradigm. Hum Pathol 2011;42:918–31.
43. McConechy MK, Ding J, Senz J, Yang W, Melnyk N, Tone AA, et al. Ovarian and endometrial endometrioid carcinomas have distinct CTNNB1 and PTEN mutation profiles. Mod Pathol 2014;27:128–34.

44. Wiedemeyer K, Wang L, Kang EY, Liu S, Ou Y, Kelemen LE, et al. Prognostic and theranostic biomarkers in ovarian clear cell carcinoma. Int J Gynecol Pathol 2022;41:168–79.
45. Sieh W, Kobel M, Longacre TA, Bowtell DD, deFazio A, Goodman MT, et al. Hormone-receptor expression and ovarian cancer survival: an ovarian tumor tissue analysis consortium study. Lancet Oncol 2013;14:853–62.
46. Wang L, Rambau PF, Kelemen LE, Anglesio MS, Leung S, Talhouk A, et al. Nuclear beta-catenin and CDX2 expression in ovarian endometrioid carcinoma identify patients with favourable outcome. Histopathology 2019;74:452–62.
47. Min Y, Agresti A. Modeling nonnegative data with clumping at zero: a survey. Journal of the Iranian Statistical Society 2002;1:7–33.
48. Chiu DS, Talhouk A. diceR: an R package for class discovery using an ensemble driven approach. BMC Bioinf 2018;19:11.
49. Khalique S, Naidoo K, Attygalle AD, Kriplani D, Daley F, Lowe A, et al. Optimised ARID1A immunohistochemistry is an accurate predictor of ARID1A mutational status in gynaecological cancers. J Pathol Clin Res 2018;4:154–66.
50. Hao J, Yu H, Zhang T, An R, Xue Y. Prognostic impact of tumor-infiltrating lymphocytes in high grade serous ovarian cancer: a systematic review and meta-analysis. Ther Adv Med Oncol 2020;12:1758835920967241.
51. Kroeger DR, Milne K, Nelson BH. Tumor-infiltrating plasma cells are associated with tertiary lymphoid structures, cytolytic T-cell responses, and superior prognosis in ovarian cancer. Clin Cancer Res 2016;22:3005–15.
52. Karanikas V, Speletas M, Zamanakou M, Kalala F, Loules G, Kerenidi T, et al. Foxp3 expression in human cancer cells. J Transl Med 2008;6:19.
53. Chen GY, Chen C, Wang L, Chang X, Zheng P, Liu Y. Cutting edge: broad expression of the FoxP3 locus in epithelial cells: a caution against early interpretation of fatal inflammatory diseases following in vivo depletion of FoxP3-expressing cells. J Immunol 2008;180:5163–6.
54. Yang S, Liu Y, Li MY, Ng CSH, Yang SL, Wang S, et al. FOXP3 promotes tumor growth and metastasis by activating Wnt/beta-catenin signaling pathway and EMT in non-small cell lung cancer. Mol Cancer 2017;16:124.
55. Hinz S, Pagerols-Raluy L, Oberg HH, Ammerpohl O, Grussel S, Sipos B, et al. Foxp3 expression in pancreatic carcinoma cells as a novel mechanism of immune evasion in cancer. Cancer Res 2007;67:8344–50.
56. Webb JR, Milne K, Kroeger DR, Nelson BH. PD-L1 expression is associated with tumor-infiltrating T cells and favorable prognosis in high-grade serous ovarian cancer. Gynecol Oncol 2016;141:293–302.
57. Zhang S, Minaguchi T, Xu C, Qi N, Itagaki H, Shikama A, et al. PD-L1 and CD4 are independent prognostic factors for overall survival in endometrial carcinomas. BMC Cancer 2020;20:127.
58. Blagih J, Zani F, Chakravarty P, Hennequart M, Pilley S, Hobor S, et al. Cancer-specific loss of p53 leads to a modulation of myeloid and T cell responses. Cell Rep 2020;30:481–96.
59. Shi Y, Xie T, Wang B, Wang R, Cai Y, Yuan B, et al. Mutant p53 drives an immune cold tumor immune microenvironment in oral squamous cell carcinoma. Commun Biol 2022;5:757.
60. Montfort A, Pearce O, Maniati E, Vincent BG, Bixby L, Bohm S, et al. A strong B-cell response is part of the immune landscape in human high-grade serous ovarian metastases. Clin Cancer Res 2017;23:250–62.
61. Laumont CM, Banville AC, Gilardi M, Hollern DP, Nelson BH. Tumour-infiltrating B cells: immunological mechanisms, clinical impact and therapeutic opportunities. Nat Rev Cancer 2022;22:414–30.
62. Zheng L, Qin S, Si W, Wang A, Xing B, Gao R, et al. Pan-cancer single-cell landscape of tumor-infiltrating T cells. Science 2021;374:abe6474.
63. Tay RE, Richardson EK, Toh HC. Revisiting the role of CD4(+) T cells in cancer immunotherapy-new insights into old paradigms. Cancer Gene Ther 2021;28:5–17.
64. Smith D, Stewart CJR, Clarke EM, Lose F, Davies C, Armes J, et al. ER and PR expression and survival after endometrial cancer. Gynecol Oncol 2018;148:258–66.
65. Bosse T, Powell M, Crosbie E, Leary A, Kroep J, Han K, et al. 595 Implementation of collaborative translational research (TransPORTEC) findings in an international endometrial cancer clinical trials program (RAINBO). Int J Gynecol Cancer 2021;31:A108–9.